

1 **i) Scaling up experimental ocean acidification and warming research: from individuals**  
2 **to the ecosystem**

3 **ii) OAW: from individuals to the ecosystem**

4 **iii)** Ana M. Queirós\*<sup>1</sup>, José A. Fernandes<sup>1</sup>, Sarah Faulwetter<sup>2</sup>, Joana Nunes<sup>1</sup>, Samuel P. S.  
5 Rastrick<sup>3,4</sup>, Nova Mieszowska<sup>5</sup>, Yuri Artioli<sup>1</sup>, Andrew Yool<sup>6</sup>, Piero Calosi<sup>3</sup>, Christos  
6 Arvanitidis<sup>2</sup>, Helen S. Findlay<sup>1</sup>, Manuel Barange<sup>1</sup>, William W. L. Cheung<sup>7</sup> and Stephen  
7 Widdicombe<sup>1</sup>

8 **iv)**

9 <sup>1</sup>Plymouth Marine Laboratory, PL1 3DH Plymouth, UK

10 <sup>2</sup>Hellenic Centre for Marine Research, Heraklion, 710 03 Crete, Greece

11 <sup>3</sup>Marine Biology and Ecology Research Centre, Plymouth University, PL4 8AA Plymouth,  
12 UK

13 <sup>4</sup>Univeristy of Southampton, SO17 1BJ Southampton, UK

14 <sup>5</sup>Marine Biological Association of the United Kingdom, PL1 2PB Plymouth, UK

15 <sup>6</sup>National Oceanography Centre, SO14 3ZH Southampton, UK

16 <sup>7</sup>Fisheries Centre, University of British Columbia, V6T 1Z4 Vancouver, Canada

17

18 **v)** \*Corresponding author. Phone: +44(0)1752633476; fax: +44(0)1752633101; email:  
19 [anqu@pml.ac.uk](mailto:anqu@pml.ac.uk).

20

21 **vi)** *Keywords:* climate change; dynamic bioclimatic envelope model; IPCC; mesocosm; ocean  
22 acidification; tomography; trophic interaction; warming.

23

24 **vii)** Type of paper: Primary Research Article

## 25 **Abstract**

26 Understanding long-term, ecosystem-level impacts of climate change is challenging because  
27 experimental research frequently focuses on short-term, individual-level impacts in isolation.  
28 We address this shortcoming first through an inter-disciplinary ensemble of novel  
29 experimental techniques to investigate the impacts of 14-month exposure to ocean  
30 acidification and warming (OAW) on the physiology, activity, predatory behaviour and  
31 susceptibility to predation of an important marine gastropod (*Nucella lapillus*). We  
32 simultaneously estimated the potential impacts of these global drivers on *N. lapillus*  
33 population dynamics and dispersal parameters. We then used these data to parameterise a  
34 dynamic bioclimatic envelope model, to investigate the consequences of OAW on the  
35 distribution of the species in the wider NE Atlantic region by 2100. The model accounts also  
36 for changes in the distribution of resources, suitable habitat and environment simulated by  
37 finely resolved biogeochemical models, under three IPCC global emissions scenarios. The  
38 experiments showed that temperature had the greatest impact on individual level responses,  
39 while acidification has a similarly important role in the mediation of predatory behaviour and  
40 susceptibility to predators. Changes in *Nucella* predatory behaviour appeared to serve as a  
41 strategy to mitigate individual level impacts of acidification, but the development of this  
42 response may be limited in the presence of predators. The model projected significant large-  
43 scale changes in the distribution of *Nucella* by the year 2100 that were exacerbated by rising  
44 greenhouse gas emissions. These changes were spatially heterogeneous, as the degree of  
45 impact of OAW on the combination of responses considered by the model varied depending  
46 on local environmental conditions and resource availability. Such changes in macro-scale  
47 distributions cannot be predicted by investigating individual level impacts in isolation, or by  
48 considering climate stressors separately. Scaling up the results of experimental climate

49 change research requires approaches that account for long-term, multi-scale responses to  
50 multiple stressors, in an ecosystem context.

## 51 **Introduction**

52 Future oceans will challenge marine organisms with a multitude of ecosystem-level stressors  
53 associated with global environmental change (Byrne *et al.*, 2013). Increased atmospheric CO<sub>2</sub>  
54 concentrations will both decrease the ocean pH (i.e. ocean acidification) and the saturation of  
55 carbonated minerals, disrupting marine carbonate chemistry as well as increasing sea  
56 temperature (Doney *et al.*, 2009, Feely *et al.*, 2004, Harvey *et al.*, 2013, Kroeker *et al.*, 2013).  
57 Biological responses to Ocean Acidification and Warming (OAW) are thought to depend on a  
58 number of physiological and life history attributes at larval, juvenile and adult stages, such as  
59 their dependence on (and type of) calcifying structures, and their ability for acid-base  
60 regulation (Kroeker *et al.*, 2013). These responses depend on physiological trade-offs, that is,  
61 the transformation and allocation of energy in an organism, determining its demand for  
62 resources, and constraining the allocation to vital cellular functions that contribute to  
63 organismal performances, survival, and fitness (Brown *et al.*, 2004, Findlay *et al.*, 2011).  
64 Predicting long-term ecosystem-level responses of individual species is, however, difficult  
65 because experimental climate change research often focuses on single, short-term, species  
66 level responses in isolation (Kroeker *et al.*, 2013). What's more, long-term responses are  
67 confounded by the ability to adjust and adapt life-history patterns, both of which vary  
68 between species and populations (Eliason *et al.*, 2011). Further, inter-specific interactions  
69 may regulate high-level impacts of climate change (Harley, 2011), but have received less  
70 attention than single-species impacts in the last decade (Wernberg *et al.*, 2012). Individual-  
71 based responses of single species alone are thus unlikely to provide a sufficient basis to  
72 understand long-term responses in complex ecological environments, where species also  
73 interact (Harley, 2011). The response of a population to a changing environment further  
74 depends on other processes that operate at different scales, including modifications of  
75 behaviour, dispersal and population dynamics (Pörtner & Knust, 2007). These depend also

76 on the availability of habitat and resources necessary to support life (Thomsen *et al.*,  
77 2013), which are driven by environmental conditions varying in space and time.

78

79 Biogeochemical ecosystem models are mathematical descriptions of ecosystem processes,  
80 that capture essential rates and flows of matter and energy in space and time, and link them to  
81 the environment and biota. These can be used to project the bulk properties of ecosystems  
82 (Allen *et al.*, 2010) into the future and the past. These models therefore provide a holistic  
83 view of ecosystems where large scale research questions about global climate change can be  
84 addressed (Artioli *et al.*, 2014). However, the integration of detailed, species-level  
85 experimental information into these macro-scale applications has been limited, because these  
86 models operate at much larger spatial and temporal scales and because, for practical reasons,  
87 they typically include only very generic descriptions of species (Anderson, 2005). Such  
88 integration requires the use of a different type of macro-scale models that can use large-scale  
89 environmental patterns, as projected by biogeochemical ecosystem models, and merge it with  
90 finer mechanistic descriptions of individual species responses to that environment (Jørgensen  
91 *et al.*, 2012). Dynamic bioclimatic envelope modelling (DBEM) enables this approach  
92 (Cheung *et al.*, 2011, Fernandes *et al.*, 2013). In DBEMs, the impacts of environmental  
93 stressors on important aspects of species ecology like physiology, population dynamics,  
94 dispersal, trophic interactions and resource use (i.e. species traits) are considered  
95 simultaneously, and can be constrained using experimental or literature derived information  
96 gathered at the species-level. This information is complemented by observational species  
97 habitat preference data, and macro-scale biogeochemical simulations of environmental  
98 conditions and resource availability (i.e. primary production), to project the corresponding  
99 changes in macro-scale species distributions (Cheung *et al.*, 2011, Kearney & Porter, 2009).  
100 This framework therefore has the potential to overcome the limitations of previous

101 methodologies, and significantly enhance the way in which the necessary, detailed, species-  
102 level experimental climate change research is integrated, interpreted, and used in ecosystem  
103 level applications.

104

105 Here, we used a variety of novel techniques to quantify long-term impacts of OAW on  
106 species level physiology and trophic interactions of the dogwhelk *Nucella lapillus* (Linnaeus,  
107 1758), a species that exerts strong influence in temperate rocky-shore ecosystems through  
108 top-down controls (Trussell *et al.*, 2003 and references therein). *Nucella* preys on barnacles  
109 and mussels, foundation species that modify 3D habitat complexity, providing shelter to other  
110 species, facilitating the development of algal canopies, and therefore the recruitment of other  
111 fauna (Menge & Branch, 2001). *Nucella* predators like the crab *Carcinus maenas* (Leach  
112 1814) also exert indirect controls on the abundance of *Nucella* prey species *via* trophic  
113 cascades (Trussell *et al.*, 2003). These are key mechanisms for the maintenance of  
114 biodiversity in temperate rocky-shores. Thus, investigating how the predatory activity of  
115 *Nucella* and its vulnerability to predators are modified by global stressors is key to  
116 understanding and predicting how rocky-shore systems may change in a near-future. In order  
117 to do so, we measured *Nucella*'s response to five scenarios of OAW after a 14 month long  
118 mesocosm experiment, thus avoiding artefacts caused by shock responses to stressors  
119 observed in short-term experiments (Form & Riebesell, 2012). We measured changes in  
120 *Nucella*'s resting oxygen consumption (a proxy for metabolic rate in heterotrophs, the  
121 energetic cost of living, Brown *et al.*, 2004) and basal activity (i.e. motor activity in the  
122 absence of stimuli). These two parameters were used to verify the presence of functional  
123 trade-offs, which were expected to be negatively affected by energetic expenditure associated  
124 with increased energy cost due to exposure to acidified conditions (Calosi *et al.*, 2013, Parker

125 *et al.*, 2013) and up-regulation of metabolism by warming (Brown *et al.*, 2004). We then  
126 investigated how these individual level responses related to the wider ecology of *Nucella*, by  
127 measuring trophic interactions relevant at the community level: predatory behaviour and  
128 vulnerability to predation. First, we monitored the behavioural response of *Nucella* to a prey  
129 mimic made of fresh tissues of a prey species (the mussel *Mytillus edulis*, Linnaeus 1758)  
130 using time-lapse photography and digital tracking techniques. Second, as the shell of *Nucella*  
131 is its main defence against predators (Crothers, 1985), we used micro-computer-aided  
132 tomography (“microCT”) to quantify changes in shell integrity as a proxy for its vulnerability  
133 to predation. We complemented these observations with an assessment of the impacts of the  
134 long-term experimental treatments on other parameters associated with the wider population  
135 dynamics of the species, such as growth and mortality. Finally, we used these results to  
136 parameterize, for the first time, a size-spectrum based DBEM (SS-DBEM, Fernandes *et al.*,  
137 2013). This enabled us to scale-up our species-level experimental results, by modelling how  
138 the combination of all the ecologically relevant measured responses to OAW may impact on  
139 the distribution and abundance of *Nucella lapillus* in the broader NE Atlantic region, by the  
140 year 2100. The biogeochemical models used by the SS-DBEM were forced using three global  
141 emissions scenarios from the 4<sup>th</sup> and 5<sup>th</sup> IPCC Assessment Reports (IPCC, 2007, IPCC, 2013)  
142 to simulate three possible degrees of future global change. The projected *Nucella*  
143 distributions in each scenario were expected to reflect the local impacts of changing abiotic  
144 parameters and resource availability over time, given that the low dispersal potential of this  
145 species (i.e. low mobility and direct development, Crothers, 1985) would likely limit its  
146 ability to track possible changes in the distribution of suitable habitat. The diversity of data  
147 and techniques used here was therefore expected to provide a more complete assessment of  
148 how species-level impacts of acidification and warming may propagate across to community  
149 and ecosystem scales, than could be predicted from individual-level responses alone.



150 **Materials and Methods**

151

152 *Mesocosm setup and experimental exposures*

153 *Nucella lapillus* individuals were collected from the low intertidal and sub-tidal fringe of the  
154 rocky-shore in Mount Batten, in the Plymouth Sound (N 50° 21' 30.29", E -4° 7' 50.07") in  
155 January 2011. All individuals were immediately transported to the PML Intertidal Mesocosm  
156 Acidification System (PML-IMAS) within one hour of collection, where they were initially  
157 allowed to acclimate to laboratorial conditions in ambient seawater, pH and temperature, for  
158 approximately three weeks. Experimental exposure was initiated in February 2011, and lasted  
159 14 months. A detailed description of the mesocosm setup and monitoring parameters for  
160 temperature, salinity, pH, total alkalinity, inorganic nutrients and associated calculated  
161 carbonate system parameters can be found in Findlay *et al.* (2013) and Table SI. In summary,  
162 the PML-IMAS consists of twenty 1 m<sup>3</sup> mesocosm tanks (700 L of seawater and 300 L of  
163 overlying atmosphere) set up in four rows of five. Five experimental treatments were  
164 haphazardly allocated between the 20 tanks, with four replicate tanks *per* treatment. The PML  
165 -IMAS uses a pump and ballast system to simulate a semi-diurnal tidal cycle that followed  
166 the monthly local conditions in the Plymouth Sound during the exposure period. The day-  
167 night light cycle was simulated to replicate the average amount of hours for each month.  
168 Each tank had an individual recirculating pumping and filtration system.

169

170 The experimental treatments used corresponded to three CO<sub>2</sub> concentration treatments at  
171 ambient temperature, i.e. the “ambient” treatments: 380, 750 and 1000 ppm; and two CO<sub>2</sub>  
172 concentration treatments at ambient temperature plus 2°C, i.e. the “warm” treatments: 380

173 and 750 ppm. Forty-two individuals were haphazardly allocated to each tank, after the initial  
174 acclimation period and once experimental conditions had stabilized. Potential shock effects  
175 caused by this non-gradual transition into experimental conditions were expected to have  
176 been overcome after more than one year of exposure to experimental conditions, when the  
177 measurements were conducted. The mesocosm laboratory is a temperature controlled room  
178 that was set so that the seawater temperature in the ambient temperature treatment tanks  
179 followed the average monthly sea surface temperature variability at the Western Channel  
180 Observatory L4 station, in the Plymouth Sound (fig. S1). These conditions were seen to be a  
181 good representation of the bulk temperature variability at the site where the animals were  
182 collected. Warm temperature treatments were further regulated by use of 300 W immersion  
183 heaters in individual tanks. The level of acidification in each tank was regulated using a pre-  
184 mixed gas system modified from Findlay *et al.* (2008). In brief, the desired atmospheric CO<sub>2</sub>  
185 concentration was created by mixing pure CO<sub>2</sub> gas with CO<sub>2</sub>-free air using flow meters and  
186 mixing vessels, monitored with a closed path CO<sub>2</sub> analyser (820, Li-Cor). Each mesocosm  
187 tank was bubbled with the desired air or CO<sub>2</sub>-air mix, and the seawater was allowed to reach  
188 equilibrium. Loss of CO<sub>2</sub> from the overlying “atmosphere” was minimised by thick PVC  
189 covers positioned over each tank and effectively separating the tank atmosphere from the  
190 room atmosphere. The pH in the control treatments was maintained as closely as possible to  
191 the yearly mean pH at L4 (2008-2012), i.e. pH = 8.08 ± 0.07 (mean ± SD), *via* regulation of  
192 the CO<sub>2</sub> concentration as above. During the emersion periods, *N. lapillus* individuals were  
193 exposed to the desired CO<sub>2</sub> atmosphere and during immersion the organisms were exposed to  
194 sea water which had adjusted its carbonate chemistry in response to the atmospheric CO<sub>2</sub>  
195 conditions. Therefore, the experimental treatments exposed our animals to some degree of  
196 daily variability in pH and temperature associated with the experimental semi-dial tidal  
197 cycles that may be seen as a bulk representation of this variability in a true intertidal rocky-

198 shore. Further variability associated with inter-tidal micro-habitats (Helmuth & Hofmann,  
199 2001) would have been difficult to standardize across replicates, and possibly deter from our  
200 ability to test the impact of our main experimental treatments.

201

### 202 *Activity and predatory behaviour assessment setup*

203 Fourteen months after the beginning of the mesocosm exposures, the basal activity and  
204 predatory behaviour of two groups of three individuals from each tank were assessed. The  
205 assessment setup consisted of individual 12 x 12 x 40 cm transparent acrylic tanks  
206 (“assessment tanks”), enclosing a water layer of approximately 35 cm (0.5 L), and a 5 cm  
207 atmosphere (0.07 L). Each tank was placed at one end of a closed 35 x 64 x 90 cm wooden  
208 black box, illuminated with an 8 W light. Within each box, at the opposite end, a digital SLR  
209 camera (Canon EOS 500 D, 15 MP) was setup to be remotely controlled *via* a PC, using the  
210 time-lapse photography software EOS GB time-lapse. The camera enabled the recording of  
211 individual behaviour during the assessments (focal distance = 70 cm). Water conditions were  
212 manipulated in individual header tanks to reflect those in the mesocosm system in which the  
213 individuals had been maintained during the previous 14 months, and supplied to the  
214 assessment tanks at approximately 40 mL min<sup>-1</sup> *via* a peristaltic pump system. In each header  
215 tank, regulation of temperature was achieved by use of 100 W immersion heaters. The pH  
216 was regulated by gentle bubbling of the desired air (or CO<sub>2</sub>-air mix described above) in  
217 header tanks and in the assessment tanks, using small aquaria diffusing stones. A closed re-  
218 circulation system maintained conditions constant throughout each assessment.

219

### 220 *Behavioural assessments*

221 During each assessment (see fig. S2), a randomly selected group of three animals from each  
222 tank ( $n_{\text{groups total}} = 40$ ;  $n_{\text{groups per treatment}} = 8$ ) was gently lowered to the bottom of the  
223 assessment tanks by use of a device made out of nylon mesh and wire, ensuring minimum  
224 direct manipulation and disturbance of individuals. Each black box was immediately closed,  
225 sheltering individuals from any disturbance related to the presence of observers. Time-lapse  
226 recording of images was initiated immediately, and carried out at five minute intervals for  
227 three hours ( $n_{\text{images per assessment}} = 36$ ). The assessment of individual groups was randomized  
228 across treatments over time to avoid confounding of observed behaviours and mesocosm  
229 exposure length, as only two groups could be assessed per day. Randomization was achieved  
230 using the random number generator package “random” for R (R Foundation for Statistical  
231 Computing, Vienna, Austria). Individuals would typically reposition themselves onto the  
232 waterline as soon as they were introduced to the assessment tanks, as observed by others  
233 (Vadas *et al.*, 1994). Basal activity was therefore measured through the quantification of the  
234 overall speed of individuals during their trajectory to the water line at the top of the  
235 assessment tank. This behaviour was assessed for 3 hours, as this period has been found to be  
236 more than sufficient for individual *N. lapillus* to adjust to the experimental setup and carry  
237 out a decision process as to where to place themselves within it (Vadas *et al.*, 1994). Because  
238 the presence of one animal in this area appeared to influence the speed and direction of other  
239 animals in choosing a location in the tank, “basal activity” henceforth refers to the  
240 measurement of the ratio of the distance to time (i.e. “speed”) of the first animal to reach the  
241 waterline in each assessment. When that animal reached the waterline, movement was  
242 recorded only for the time elapsed until then. When all animals failed to reach the waterline  
243 during the assessment period, all movements were recorded over the three hours, and basal  
244 activity (time and distance, to calculated speed) considered for the individual that initiated  
245 movement first. At the end of the activity assessment (3 hours) a prey mimic was gently

246 lowered to the bottom of the assessment tank, using a mesh device as before to minimize  
247 interference. The response of individuals to this prey mimic was investigated as a proxy for  
248 predatory behaviour. The mimic consisted of a bag of approximately 10 g of fresh live  
249 mussels (*Mytillus edulis*, Linnaeus 1758), which were manually crushed and immobilized  
250 within a closed double mesh bag immediately prior to the assessment. This standardization of  
251 the prey mimic was required to avoid confounding of the responses associated with a choice  
252 of prey based, for example, on prey size (Crothers, 1985). The prey mimic was placed near  
253 the diffusing air stone in each assessment tank to maximize the distribution of prey odour  
254 cues (fig. S2). “Response time” was recorded as the time taken by the first individual to reach  
255 the prey mimic, because the presence of one feeding animal appeared to deter other  
256 individuals from approaching the prey mimic. Equally, “foraging distance” was recorded as  
257 the overall length of the trajectory covered by the first individual to reach the prey mimic.  
258 “Handling time” was calculated as the time during which individual animals were observed  
259 directly manipulating the mesh bag containing the prey mimic. When no individuals were  
260 able to find the position of the prey mimic, the trajectory considered was that of the most  
261 active individual, for all responses to prey. As difficulty in locating food may be an indication  
262 of limited chemo-sensory function that has been observed in polychaetes (Schaum *et al.*,  
263 2013), crabs (de la Haye *et al.*, 2012) and fish (Cripps *et al.*, 2011, Dixon *et al.*, 2010,  
264 Johannesen *et al.*, 2012) exposed to acidification, we investigated possible mechanisms by  
265 which *Nucella* could compensate such potential limitation. To this end, we measured the ratio  
266 of foraging distance to prey handling time (“foraging cost”) as an indication of the energetic  
267 expenditure associated with foraging in relation to the energetic gain associated with feeding.  
268 This was calculated to provide an overall energetic cost-benefit metric of predatory  
269 behaviour. All assessments were timed to match the introduction of the prey mimic to dusk,  
270 when individuals were expected to be most active (Crothers, 1985). Predatory behaviour was

271 assessed for three hours after the introduction of the prey mimic, with images captured at five  
272 minute intervals ( $n_{\text{images per assessment}} = 36$ ), as before. At the end of the six hour assessments,  
273 all dog whelks were gently removed from assessment tanks, marked, and individual wet  
274 weights and lengths recorded, before returning them to the mesocosm system. Prey mimics  
275 were euthanized by freezing.

276

### 277 *Analysis of time-lapse image sequences*

278 Activity and response to the prey mimic were quantified by digital analysis of the time-lapse  
279 image sequences from each trial, using the plugin “Manual tracking”, and custom-made  
280 scripts, for the open source image analysis software Image J (1.45S, National Institutes of  
281 Health, USA). Tracking of each individual trajectory during the assessments enabled the  
282 recording of the time and length associated with behaviours here described (see fig. S2 for  
283 examples). A total of 36 image sequences were analysed *per* assessment (before and after  
284 prey cue addition,  $n_{\text{images}} = 2596$ ), excluding cases where software glitches led to image  
285 capture failure (4 out of 40 assessments were overall null). Each sequence was analysed three  
286 times, to allow the tracking of each individual in the group of three, per assessment. The four  
287 outcome variables (basal activity, i.e. speed; response time (to reach prey); foraging distance;  
288 foraging cost) were analysed separately using multiple regression and a log-likelihood based  
289 stepwise regression analyses for model selection in R. The CO<sub>2</sub> concentration and  
290 temperature were considered as main effects and up to first order interaction, and tidal  
291 condition at the beginning of each assessment was considered as a covariate. Normality of  
292 residuals and homoscedasticity were verified by observation of residual distributions.

293

294 *Determination of metabolic rates*

295 For heterotrophs, metabolic rate is determined using the rate of oxygen consumption as a  
296 proxy. This was measured within two weeks of the behavioural assessments, using stop-flow  
297 respirometers (volume 278 mL). Each respirometer contained 20 glass beads (diameter =  
298 1cm) to provide a replica substrate and reducing stress and activity levels. Magnetic stirrers  
299 were used to prevent the formation of oxygen partial pressure ( $pO_2$ ) gradients within the  
300 respirometers. The stirrers were separated from the animals by a perforated platform.  
301 Eighteen respirometers were used, and these were divided in to three sets of six; each set was  
302 supplied with fully oxygenated seawater from a reservoir, at the desired temperature and  $CO_2$   
303 level matching the respective mesocosm exposure conditions. During the assessment period  
304 the temperature was controlled using a recirculating water bath (Grant Cambridge Ltd,  
305 Cambridge, UK) monitored using a K type thermocouple inside the respirometers (Omega,  
306 HH806AU, Manchester, UK). This provided a water jacket housing the respirometers and  
307 cooling coils in the reservoirs. The  $CO_2$  of each reservoir was controlled using the same air  
308 and carbon dioxide gas mixes which were used to supply the mesocosm from which the  
309 animals had been taken. Sea water was filtered (2.22  $\mu m$ ) and preliminary experiments  
310 showed no significant decline in  $pO_2$  within the respirometers in the absence of the animals.  
311 Each group of three snails, previously used for the behavioural assessments, was placed in a  
312 separate respirometer and allowed to settle under the experimental conditions for 1 h. The  
313 respirometers were covered with an opaque plastic sheet to reduce light and disturbance.  
314 After 1 h, the flow of sea water through each respirometer was stopped and the decline in  $pO_2$   
315 within each closed respirometer was determined using an OxySense GEN III 5000 series  
316 oxygen analyser system (OxySense, Dallas, TX), using the method in Rastrick and Whiteley  
317 (2011). Rates of oxygen uptake were calculated as the change in  $pO_2 h^{-1}$  from the linear least-  
318 squares regression of  $pO_2$  (mbar) plotted against time (h). This was multiplied by the

319 solubility coefficient for oxygen, which was adjusted for salinity and temperature (Harvey,  
320 1955), and the volume of water within each respirometer, taking in to account the volume  
321 taken up by each animal. Whole animal values for  $\dot{M}O_2$  in  $\mu lO_2 h^{-1}$  were standardised to  
322 Standard Temperature and Pressure, Dry (STPD) and expressed as  $\mu mol O_2 h^{-1}$ . Metabolic  
323 rates were standardized by biomass, and analysed using multiple regressions and a log-  
324 likelihood based stepwise regression analyses for model selection in R, as before.

325

### 326 *Susceptibility to predators: analysis of shell integrity*

#### 327 *MicroCT scans of shells*

328 To investigate possible shell damage associated with experimental treatments four individuals  
329 were randomly selected from the ambient control (380 ppm) and the high CO<sub>2</sub> treatments  
330 (1000 ppm) (n=8) at exposure month 14. Individuals were euthanized by immersion in liquid  
331 nitrogen, after anesthesia by immersion in an 8% MgCl solution for 12 hours. Specimens  
332 were further preserved in dry-ice for air freight, and later stored at -80° C until scanning took  
333 place. Images were acquired with a SkyScan 1172 micro-computer tomograph  
334 (<http://www.skyscan.be/products/1172.htm>) at the Hellenic Centre for Marine Research  
335 (Crete, Greece). The SkyScan uses a tungsten source and is equipped with an 11 PM CCD  
336 camera (4000 × 2672 pixel), with maximal resolution of < 0.8  $\mu m pixel^{-1}$ . Specimens were  
337 scanned with a copper and aluminum filter at 100 kV, with a flux of 100  $\mu A$ , on full 360°  
338 rotation and at the highest possible camera resolution. Effective voxel size was  $5.5 \pm 0.3 \mu m^3$ .  
339 Projection images acquired during the scanning process were subsequently reconstructed into  
340 cross sections (\*.png format) with SkyScan's NRecon software which employs a modified  
341 Feldkamp's back-projection algorithm. Sections were always reconstructed from the total  
342 number of projection images (360°) to maximize detail. Parameters were calibrated between



343 acquired image sets to insure data comparability between individuals – this procedure is  
344 hence forth referred to as inter-calibration. The lower limit of the histogram was set at the  
345 value of the sample surrounding medium during scans (i.e. air).

346

#### 347 *Analysis of microCT data*

348 Possible changes in shell density associated with experimental treatments were likely to be  
349 more clearly observed in the growing (or newer) edge of shells. Analysis of shell data was  
350 therefore primarily centred on image slices corresponding to the upper lip area (top line, fig.  
351 S3), where the shell was newer and thinner. This area is henceforth referred to as “lip”. Shell  
352 damage was also likely to be observed on the surface of shells which, in the absence of a  
353 periostracum, were directly exposed to experimental seawater conditions (Rodolfo-Metalpa *et*  
354 *al.*, 2011). Possible changes to the shell surface were therefore investigated focusing on a  
355 0.08 mm deep layer on the surface of each scanned individual. To achieve this, 10 microCT  
356 slices corresponding to cross-sections of shells were acquired in the same specific regions of  
357 each scanned individual as illustrated in fig. S3. This choice insured a good and comparable  
358 coverage of the whole shell between individuals. In each slice, a 15 pixel thick region of  
359 interest below the surface of the shell was hand drawn in Image J (pixel size = 5.5  $\mu\text{m}$ ). This  
360 region is referred to as the “shell surface” in subsequent analysis. The density of the shell  
361 surface in each individual was calculated using as a proxy the mean pixel intensity in that  
362 region (0 to 255, with high values indicating higher density), across all ten 2D slices, which  
363 had been inter-calibrated during reconstruction. The density of the shell in the lip was  
364 calculated in the same way, using the whole 2D slice corresponding to that region.  
365 Differences in density in each of the parameters (lip and shell surface) between controls and  
366 animals from the 1000 ppm CO<sub>2</sub> treatment were compared using one-tailed t-tests. The tests

367 assumed normality and equal variances, as verified *via* Shapiro-Wilk tests and plotting of  
368 data dispersion, and used the alternative hypothesis that shell density in the high CO<sub>2</sub>  
369 treatment was lower. All data analyses were carried out in R.

370

### 371 ***Projection of ecosystem-level changes in biogeography***

372 The size-spectrum dynamic bioclimatic envelope model (SS-DBEM) described in Fernandes  
373 *et al.* (2013) was used here to project possible changes in biogeography associated with ocean  
374 acidification and warming. The SS-DBEM couples the DBEM described by Cheung *et al.*  
375 (2011) with a size-spectrum model for resource use based on primary production and  
376 temperature (Jennings *et al.*, 2008). The SS-DBEM combines a correlative habitat suitability  
377 component with a mechanistic niche component (Kearney & Porter, 2009) to project  
378 environmental limits to species distributions, as a result of a transference of the realized  
379 species niche (as constrained by the experimental data) to the landscape scale (i.e. the NE  
380 Atlantic). Specifically, the correlative habitat suitability component of the model maps out  
381 species occurrence to environmental patterns (temperature, depth, substrate type etc.) based  
382 on global databases (e.g. sealifebase.org). We complemented this with *N. lapillus*  
383 distributional data from the Marine Biological Association of the UK's MarClim project  
384 (Mieszkowska *et al.*, *In press*). These were used to define the environmental tolerance range  
385 for the species (i.e. its habitat preference profile) based on a set of "filters", including habitat  
386 type, depth and latitudinal limits (Close *et al.*, 2006). Current geographic distribution is  
387 predicted based these filters. Temperature was not used here as a predictor of current  
388 distribution because it was later used to estimate the temperature tolerance and preference of  
389 the species (Cheung *et al.*, 2008). On its own, this approach is limited because it does not  
390 enable a distinction to be made between direct causality between environment and species

391 distribution, indirect mediation via biotic interactions, and direct response to non-modelled  
392 variables co-linear with those considered by the model (Kearney & Porter, 2009, Mac Nally,  
393 2000). Therefore, in addition, the model also includes a mechanistic niche component by  
394 which the projected species distribution becomes limited by more factors than just the  
395 distribution of suitable habitat. In the mechanistic niche component, change in distribution  
396 and relative abundance (and biomass) caused by changing environmental conditions are  
397 simulated by a spatial population dynamic model (Cheung et al. 2011). The spatial and  
398 temporal dynamic model is dependent on a set of physiological and ecological response traits,  
399 constrained in this case by responses to acidification and temperature observed during the  
400 mesocosm experiments, which are used to determine persistence at the meta-population level.  
401 In the present study, the model considered changes in resting oxygen consumption (a proxy  
402 for metabolic rate), adult mobility (i.e. speed, as a proxy for dispersal potential), growth,  
403 length-weight relationship (a proxy for condition), adult and juvenile mortality, and larval  
404 dispersal, as measured in response to temperature and acidification. These traits were  
405 calculated per treatment level. Change in resting oxygen consumption with temperature (eV)  
406 and mobility (i.e. cm.h<sup>-1</sup>) were calculated at 14 months based on the mesocosm measurements  
407 already described. Mortality of adults and juveniles (F1 hatched in the laboratory from the  
408 same adults described above) was calculated as an overall % *per* treatment, based on the 14  
409 month mesocosm experiments. Larval dispersal was considered to be negligible as *N. lapillus*  
410 is a direct developer. Growth rates were calculated as the difference (%) in weight increment  
411 (g day<sup>-1</sup>) between each treatment and the control (ambient temperature and 380 ppm of CO<sub>2</sub>),  
412 superimposed on the von Bertalanffy growth equations for *Nucella* in Selin (2010). Growth  
413 and length-weight relationships were calculated here using data generated by a parallel 12  
414 month experiment on individuals of the same wild population, which used the same  
415 experimental treatment levels and supporting equipment, carried out in the mesocosm

416 facilities of the Marine Biological Association of the UK. A schematic diagram of the model  
417 structure and input parameters is illustrated in figure S4.

418 The environmental forcing for the SS-DBEM (i.e. the environmental parameters, or habitat  
419 conditions) was projected for the NE Atlantic region using two spatially and temporally  
420 resolved biogeochemical models: the Proudman Oceanographic Laboratory Coastal Ocean  
421 Modelling System – European Regional Seas Ecosystem Model (POLCOMS-ERSEM), and  
422 the Nucleus for European Modelling of the Ocean – Model of Ecosystem Dynamics, nutrient  
423 Utilisation, Sequestration and Acidification (NEMO-MEDUSA 2.0) documented in Artioli *et*  
424 *al.* (2014) and Yool *et al.* (2013). POLCOMS-ERSEM has a track record for performance in  
425 regional seas (Allen & Somerfield, 2009, Shutler *et al.*, 2011), while NEMO-MEDUSA is a  
426 large-scale global ocean model. Together, they therefore provided a complimentary approach  
427 to the simulation of biogeochemical conditions. The two models were parameterized  
428 according to three global emissions scenarios (IPCC, 2007, IPCC, 2013) to simulate three  
429 possible futures for *Nucella*. The future emissions scenarios considered were: 1) AR4 A1B  
430 with a CO<sub>2</sub> equivalent around 700 ppm (“business-as-usual” , IPCC, 2007); 2) AR5 RCP2.6  
431 with a CO<sub>2</sub> equivalent around 400 ppm (“lower emissions” , IPCC, 2013); and 3) AR5  
432 RCP8.5 with a CO<sub>2</sub> equivalent around 1250 ppm (“higher emissions” , IPCC, 2013). In each  
433 case, the SS-DBEM was forced for a specific 20 year biogeochemical simulation  
434 corresponding to present time (1981-2000) and end of the century (2081-2100). The first five  
435 year spin-off period was discarded from further analysis while the subsequent fifteen years  
436 were averaged to account for the expected inter-annual natural variability. The  
437 biogeochemical model runs simulate not only the landscape-scale habitat conditions  
438 (including temperature and pH) but also the resources available in each point in time and  
439 space. I.e., primary production (as simulated by the biogeochemical models) and the  
440 predicted habitat suitability from other environmental factors were used as a proxy for the

441 carrying capacity of the ecosystem at each point. For a set group of neighbouring points at  
442 each specific time point, the SS-DBEM simulates that *Nucella* will use more resources from  
443 primary production where habitat is more suitable. The SS-DBEM was parameterized using  
444 the measured changes in *Nucella* traits in relation to the CO<sub>2</sub> concentration and temperature  
445 levels observed in the experimental treatments. When no statistically significant differences  
446 were found between treatments, model parameters were calculated as the overall mean value  
447 for each measured trait.

448 In each of the three IPCC scenarios used, we ran the SS-DBEM three times, allowing model  
449 parameters to vary according to acidification, warming or both effects, using all of our  
450 experimental trait data simultaneously. These runs were compared to highlight potentially  
451 distinct effects of acidification and warming in the diversity of parameters considered by the  
452 SS-DBEM. The final SS-DBEM model grid had a 0.5 ° latitude by 0.5 ° longitude resolution  
453 (approximately 56 km<sup>2</sup> depending on latitude). Detailed descriptions of the models used are  
454 found in Cheung *et al.* (2011) and Fernandes *et al.* (2013).

## 455 **Results**

456

### 457 ***Impacts on resting oxygen consumption and basal activity***

458 Ocean acidification and warming had distinct effects in the resting oxygen consumption of  
459 *Nucella* (here used as proxy for metabolic rate). At ambient temperature, resting oxygen  
460 consumption (MO<sub>2</sub>) decreased steadily with increased CO<sub>2</sub> exposure, but in warm treatments  
461 this parameter was significantly higher and invariable with CO<sub>2</sub> concentration: MO<sub>2</sub> = 16.95  
462 + 6.33 x temperature - 0.01 x CO<sub>2</sub>, R<sup>2</sup> = 78.49 % with F<sub>2,25</sub> = 45.63 and p < 0.01, fig. 1a.  
463 This pattern of impact was only partially mirrored in individual basal activity (i.e. speed, fig.

464 1b, for which the univariate regression using metabolic rate as a predictor yielded  $R^2 = 78.49$   
465 %,  $F_{1,9} = 4.39$  and  $p < 0.10$ ). Acidification in the absence of warming did lead to decreased  
466 activity, but under warming conditions *Nucella* was as active as in control treatments (Amb  
467 380, fig. 1b) regardless of acidification levels (fig.1b). A significant amount of variability  
468 observed between individuals could not be explained by the experimental treatments ( $R^2 =$   
469 32.15 %, table I and fig. 1b).

#### 470 ***Impacts on predatory behaviour***

471 The impact of experimental treatments on the predatory behaviour parameters measured here  
472 were significant but complex (table I, fig.1c-f). In the presence of food (prey mimic),  
473 foraging time (i.e. “response time”, table I, figure 1c) was highly variable, causing no  
474 significant impact on the mean responses across individuals. Individuals from the worst  
475 acidification scenario were, however, found to cover significantly greater distance to find  
476 food in the absence of warming (“foraging distance”, table I and fig. 1d), and this variable did  
477 not exhibit a clear pattern in other treatments, regardless of temperature. We also found that  
478 the amount of time spent feeding (“handling time”) appeared to trail the increase in distance  
479 covered to find food, despite inter-individual variation. Consequentially, a pattern emerged  
480 when foraging cost was calculated (the ratio of handling time to foraging distance). With  
481 increased acidification, and independent of temperature, an increase in the amount of time  
482 spent feeding exceeded the corresponding increase in distance covered to find prey, leading to  
483 a decrease in foraging cost (figs. 1e and f,  $p < 0.05$  and  $R^2 = 52.30$  %, table I).

484

#### 485 ***Impact on susceptibility to predation***

486 The analysis of the microCT data revealed profound changes in shell morphology concurrent  
487 with acidification (fig.2). Dissolution at the shell apex, irregular definition of whorls and the  
488 disappearance of the natural ornamentation pattern with increased acidification (3D  
489 reconstructions, fig.2) were consistent with a 20-30% decrease in shell density in the shell lip  
490 ( $t_6 = -1.80$  and  $p < 0.10$ ) and in the overall shell surface ( $t_6 = -2.32$  and  $p < 0.05$ ).

491

### 492 ***Biogeographical projections for the end of the century***

493 We used a state-of-the-art dynamic bioclimatic envelope model (SS-DBEM) to explore how  
494 the mechanisms highlighted by our species-level experimental results scaled through to the  
495 ecosystem, considering different emission scenarios and model structure. Overall, higher  
496 emissions led to greater reductions in the abundance of *Nucella lapillus* across all areas  
497 (fig.3). By 2100, the abundance of *Nucella* in the NE Atlantic shelf coasts would have  
498 decreased as an effect of OAW by  $66.9 \pm 16.8$  % (mean  $\pm$  SD) across all areas (in relation to  
499 present day), in business-as-usual and higher emissions scenarios (fig.3 a-d and i-l).  
500 Alternatively, abundance could increase marginally in the same period under a lower  
501 emissions scenario ( $1.22 \pm 0.78$  %, fig.3e-h). The response of the different species traits (i.e.  
502 model parameters) to variations in each of the stressors considered over space and time  
503 (temperature and CO<sub>2</sub>, fig. 3 b-c, f-g and j-k), or of their combination (fig. 3 d, h and l) means  
504 that the projected distributional changes are spatially heterogeneous. In the northern UK and  
505 Irish coasts, the projected decrease in abundance associated with OAW (in relation to present  
506 day) is similar for business-as-usual and higher emissions scenarios for 2100 (by  $63.58 \pm$   
507  $4.88$  %, fig.3d and l), but in all other coasts abundance may fall by an additional  $37.06 \pm$   
508  $4.88$  % in the worst scenario (fig.3h). In a future where emissions continue to occur in  
509 business-as-usual, the greatest decrease in abundance may occur in the NE coast of the UK

510 (fig. 3d), while in a higher emissions scenario, areas further south would suffer the greatest  
511 impacts (fig. 3l). In some areas of the coastline along the English Channel and in the western  
512 coast of France, smaller changes in the future distribution of *Nucella* were projected when all  
513 model parameters responded to OAW (right column, fig. 3 d, h and l) than when they  
514 responded to only one of the individual stressors (second and third columns, fig. 3 b-c, f-g  
515 and j-k), at and below business-as-usual emissions levels. In other areas, like the NE of  
516 England, the reverse was true, at and above business-as-usual emissions levels (fig. 3). The  
517 SS-DBEM projections also indicated that resource availability may be an important factor  
518 determining the extent of distributional changes over time. Specifically, the projections  
519 indicated that, with the exception of the most extreme higher emissions scenario, *Nucella*  
520 would likely be able to meet increased energetic demand associated with OAW in areas with  
521 high productivity, such as the German and Dutch coasts (fig.3d and l). However, in less  
522 productive areas, like the East coast of England, resource depletion may prevent persistence  
523 under OAW.

524

## 525 *Discussion*

526 This study shows how environmental stressors impact the ecology of individual species  
527 across several layers, and that these are not easy to summarize. Using a diverse range of  
528 experimental analyses, we provide an integrated insight into how multi-stressor impacts may  
529 be complex and distinct from those expected by the sum of single stressor impacts.  
530 Temperature appeared to be the key factor regulating basal physiology and activity, but when  
531 predator-prey interactions were considered, acidification appeared to play an important role  
532 too. Furthermore, our macro-scale modelling indicated that the aggregated responses  
533 measured at the individual level may lead to substantial change to the future distribution of



534 *Nucella* in the NE Atlantic region by 2100, with concomitant impacts for the dynamics of  
535 these rocky-shores. This distributional impact will depend on the magnitude of environmental  
536 change (i.e. emissions scenario considered). It will also depend on the future distribution of  
537 resources, and on local variation of particular stressor combinations acting on many aspects  
538 of *Nucella* ecology together.

539

540

#### 541 ***Individual level responses***

542 Our results on basal activity and resting metabolic rate lend support to the perspective that  
543 animals are able to improve survival under adverse conditions caused by acidification alone  
544 by reducing metabolism (Calosi *et al.*, 2013, Reipschläger *et al.*, 1997) and specifically during  
545 periods of zero energy gain (i.e. rest, Brown *et al.*, 2004). However, temperature appeared to  
546 have an overriding effect on both of these parameters, as with concurrent warming, no effect  
547 of acidification was apparent. Warming increased mean resting metabolic rates and lead to  
548 variable activity levels, regardless of the exposure to different levels of acidification used in  
549 this study. After fourteen months of warming, increased metabolic rates in *Nucella* may  
550 indicate an increase in energy demand to sustain basic cellular functions, which may lead to  
551 trade-offs by which, at this stage, less energy may be available to other non-vital functions  
552 (like reproduction). The identification of exactly which of those individual processes are  
553 negatively impacted by potential trade-offs would however have required further  
554 investigation. Variability in activity (a proxy for overall performance) may reflect inter-  
555 individual differences associated with higher maintenance and repair costs, as seen by others,  
556 when metabolic rates are high (Calosi *et al.*, 2013). Both results indicate that the individual  
557 level impacts of ocean acidification are significantly different when warming was also

558 considered, illustrating how responses to multi-stressor environments cannot be predicted  
559 from the analysis of individual stressor impacts alone.

560

561 ***Good prey, bad predator: bad news for rocky-shore communities***

562 We expected that *Nucella* would require more time to find prey with increased acidification,  
563 as individuals were significantly less active in these treatments. However, we found that the  
564 time needed to find food did not increase with acidification. Alternatively, we found that far  
565 greater distance was covered to find food in the worst acidification scenario, despite of  
566 temperature. Greater foraging distance may be indicative of a lowered ability of *Nucella* to  
567 locate food when CO<sub>2</sub> concentration was high, consistent with limited chemo-sensory  
568 function observed in polychaetes (Schaum *et al.*, 2013), crabs (de la Haye *et al.*, 2012) and  
569 fish (Cripps *et al.*, 2011, Dixson *et al.*, 2010, Johannesen *et al.*, 2012) exposed to  
570 acidification. We measured foraging cost (the ratio of foraging distance to prey handling  
571 time) as a means to determine whether, after 14 months, predatory behaviour had changed to  
572 compensate for this possible chemo-sensory limitation. We found that, overall, foraging cost  
573 decreased with increased acidification given that a concurrent increase in the observed  
574 amount of time spent feeding (i.e. prey handling time) far exceeded the corresponding  
575 increase in distance covered to find prey, with and without warming. Thus, the predatory  
576 behaviour of *Nucella* did appear to change after 14 months in a way that is consistent with a  
577 strategy to cope with a higher energetic expenditure associated with finding food (i.e. greater  
578 foraging distance) in acidified conditions, possibly triggered by limited chemo-sensory  
579 function. Thus, when predatory behaviour was considered, acidification appeared to be a  
580 more important regulatory factor than temperature. Considering only the responses measured  
581 in the absence of a prey mimic (i.e. resting metabolic rate and basal activity), we could have

582 over-looked this potentially significant survival strategy, and the potentially important role of  
583 ocean acidification in the overall ecology of *Nucella* in a near-future ocean.

584

585 Changes in chemo-sensory function and predatory behaviour have implications also for the  
586 susceptibility of *N. lapillus* to predators. This species is known to shorten the amount of time  
587 spent foraging outside of refuges, feeding less and choosing to feed on prey in secluded  
588 crevices, in the presence of predators (Trussell *et al.*, 2003). This predator avoidance  
589 behaviour has also been observed in other gastropods, even when exposed to acidification  
590 (Manríquez *et al.*, 2013). Predator avoidance behaviour is, however, not compatible with a  
591 need to increase feeding time to compensate the apparent higher energy expenditure  
592 associated with finding prey for a chemo-sensorially impaired *Nucella*. It is thus possible that  
593 the presence of predators in a community context may inhibit *Nucella* from developing the  
594 predatory behavioural modifications we observed in OAW conditions in our experiments. Or,  
595 if such modification of *Nucella* predatory behaviour should develop, it may lead to increased  
596 mortality by predation. Additionally, the analysis of microCT shell data indicated  
597 significantly decreased shell density in acidified treatments, which may be indicative of  
598 greater susceptibility to physical damage as a consequence of encounters with predators.  
599 Along with shell morphology, shell robustness is a key defence of *Nucella* (and other species,  
600 McDonald *et al.*, 2009) against crushing predators like crabs. In fact, stronger shells correlate  
601 with higher survival rates in *Nucella* because they require a greater energetic investment and  
602 longer handling time for breakage, both of which tend to lead the crabs away, in search of  
603 easier prey (Hughes & Elner, 1979). Thus, together, these two results paint a bleak future for  
604 *Nucella*, and suggest that significant changes may occur in temperate rocky-shore  
605 communities as a consequence of OAW. This is because *Nucella* and its predators exhibit  
606 significant influence on the abundance of mussels and canopy forming algae (Trussell *et al.*,

607 2003 and references therein), both of which are habitat-forming species that have a regulating  
608 role in controlling rocky-shore biodiversity (Bulleri *et al.*, 2002, Seed, 1996). Our findings  
609 agree with others that also found evidence for the relevance of nervous-system level impacts  
610 of ocean acidification for predator-prey interactions in rocky-shores (Watson *et al.*, 2014), but  
611 contrast with Landes & Zimmer (2012), who found no change in predator-prey interactions  
612 with OAW in a similar ecosystem. Long-term studies of the kind presented here are resource  
613 intensive, but are crucial to understand the importance of bottom-up and top-down  
614 mechanisms for the propagation of species-level impacts of climate change to community  
615 level. However, more conclusive insights might have been obtained in the present study if  
616 both prey and predator of *Nucella* had also been maintained in the same exposures, thus  
617 unravelling how their own species-level responses to OAW would have modified the  
618 predator-prey interactions. Such long-term, multi-stressor, multi-species studies will  
619 significantly help drive the field in the future, by helping to elucidate the true impacts of  
620 climate change in complex community settings.

621

### 622 *Ecosystem-level considerations*

623 Our results, combining individual based measurements, predatory behaviour, susceptibility to  
624 predation and modelling, suggest that OAW may lead to substantial, non-additive and  
625 complex changes in community dynamics of NE Atlantic rocky-shores within the next 100  
626 years. However, despite its achievements, this study identifies the challenge of predicting  
627 ecosystem level climate change impacts based on experimental studies that consider only  
628 single responses of individual species in isolation. Different stressors appeared to have  
629 greater relevance or impacts in different aspects of *Nucella* ecology, indicating that climate  
630 change impacts species across many different levels, but that these responses do not

631 necessarily follow the same trends. Our results, however, provide a more realistic  
632 representation of the true ecosystem level impacts associated with *Nucella*, because we  
633 combined a range of species and community level processes simultaneously, and summed  
634 effects were estimated using a complex modelling framework.

635

636 The importance of local scale forcing on these processes, as revealed by the analysis of the  
637 SS-DBEM projections, advises caution about the extrapolation of experimental findings on  
638 their own to investigate large scale questions, particularly when studies consider only a small  
639 number of individual level responses. For example, it would have been incorrect to assume,  
640 based only on the presently observed decrease in foraging-cost for *Nucella* with increased  
641 acidification, that the distributional range of this species will expand because average oceanic  
642 CO<sub>2</sub> concentrations are and will continue to rise. As we show, large-scale distributional  
643 changes will occur as a result of multi-stressor patterns and resources changing locally across  
644 the landscape, in a heterogeneous way. Therefore, projection of ecosystem-level  
645 consequences of climate change requires a better integration of both macro-scale and local-  
646 scale information, about biotic and abiotic drivers, and species ecology. While the SS-DEBM  
647 quantifies possible impacts on the use of resources available in the environment primarily as  
648 described by size-spectrum theory (Jennings et al. 2008), it does not account for the inter-  
649 specific relationship between *Nucella*, its prey and predators explicitly analysed here, and the  
650 responses of such relationships to climate change. On the other hand, our experiments  
651 indicate that the impact of acidification on the predatory behaviour of *Nucella* could have a  
652 significant role also in its ability to acquire food. While the present study represents a  
653 significant development in the use of individual level experimental data in an ecosystem level

654 application, future research may require future model developments that can accommodate  
655 such specific information.

656

657 The parameterization of the SS-DBEM with experimental data is challenging, requiring  
658 expertise in a diversity of subject areas to enable parameter calculation (physiology,  
659 behaviour, population dynamics) in addition to that required to run the model. It is the  
660 research taking place within those disciplines, with single and multi-stressors, that drives our  
661 understanding of the mechanisms of impact that the model aims to capture. Thus, good  
662 communication between the modeller and specialists in each of those fields of research is  
663 paramount to successful model parameterization, insuring that both model behaviour and  
664 assumptions taken are plausible. For example, our projections are based primarily on  
665 experimental and observational information gathered within one species population, which is  
666 likely adapted or acclimated to a specific set of local environmental conditions (Calosi *et al.*,  
667 2008). We considered whether it was plausible to extrapolate this knowledge to the larger  
668 geographical area considered in our simulations. The reason for this is that it is possible that a  
669 different population of the same species could have shown some degree of variability in the  
670 responses we measured (Findlay *et al.*, 2010 and references therein). Because we measured a  
671 large number of ecologically meaningful parameters, it was considered that small differences  
672 in specific responses between populations would be diluted in our integrated analysis, and  
673 thus that our extrapolation was reasonable. However, for different species and simulations, if  
674 those differences are known and sizeable, then they should be considered.

675

676 The diversity of data used here is becoming increasingly available, given that the need for  
677 long-term, multi-species, multi-stressor experimental climate change research is gaining  
678 recognition. Our inter-disciplinary approach integrates this knowledge, providing a more  
679 holistic assessment of the effects of OAW than can be derived from assessments carried out  
680 within individual disciplines. In doing so, DBEMs also enable the testing of climate impact  
681 scenarios on marine species in the context of the ecosystem, at scales that are more relevant  
682 to management than those at which empirical and experimental science tend to operate (e.g.  
683 decades c.f. a few years). Furthermore, changes in the distribution of individual species (as  
684 modelled here for *Nucella*) can be done in a multi-species context, to predict how climate will  
685 impact marine biodiversity across the land-scape (Cheung *et al.*, 2009). Biodiversity loss is  
686 perhaps an issue more easily communicated to managers and stake-holders of the marine  
687 environment than, for instance, the physiological impacts of OAW on specific species. As  
688 biodiversity underpins regulating, production, provisioning and cultural ecosystem services  
689 (Armstrong *et al.*, 2012, Raymond *et al.*, 2009), this approach may be a successful route to  
690 scale experimental climate change research to the wider socio-economic context. Thus, as  
691 noted also by others (Metcalfé *et al.*, 2012, Norman-López *et al.*, 2013) it is timely for  
692 physiologists, ecologists and numerical modellers to take advantage of such integrative routes  
693 to increase the impact of experimental climate change science, beyond speciality fields.

694

## 695 **Acknowledgements**

696 The authors are grateful to two anonymous reviewers and the subject editor for thorough and  
697 constructive criticism received during the peer-review, which greatly improved this  
698 manuscript. AMQ, JAF, JN, SPSR, NM, YA, AY, PC, HSF, MB and SW were funded by the  
699 NERC UK Ocean Acidification Research Programme. WWLC was funded by the National

700 Geographic Society, the Nippon Foundation-Nereus Program, and Natural Sciences and  
701 Engineering Research Council of Canada. SF and CA were funded by the FP7 programme  
702 MARBIGEN. Various staff and students are thanked for help with the maintenance of the  
703 mesocosm facilities and animal husbandry at Plymouth Marine Laboratory, and at the Marine  
704 Biological Association of the United Kingdom. Michael T Burrows is thanked for initial  
705 advice about *Nucella lapillus* ecology. Alexander Langley is thanked for reviewing the  
706 manuscript.

707



## 708 References

- 709 Allen J, Aiken J, Anderson TR *et al.* (2010) Marine ecosystem models for earth systems applications:  
 710 The MarQUEST experience. *Journal of Marine Systems*, **81**, 19-33.
- 711 Allen J, Somerfield P (2009) A multivariate approach to model skill assessment. *Journal of Marine*  
 712 *Systems*, **76**, 83-94.
- 713 Anderson TR (2005) Plankton functional type modelling: running before we can walk? *Journal of*  
 714 *Plankton Research*, **27**, 1073-1081.
- 715 Armstrong CW, Holen S, Navrud S, Seifert A (2012) The Economics of Ocean Acidification—a  
 716 scoping study. Frams Center, Norway. <http://www.framsenteret.no/theeconomics-of-ocean-acidification-a-scoping-study>.
- 717
- 718 Artioli Y, Blackford J, Nondal G *et al.* (2014) Heterogeneity of impacts of high CO<sub>2</sub> on the North  
 719 Western European Shelf. *Biogeosciences Discussions*, **11**, 601-612.
- 720 Brown JH, Gillooly JF, Allen AP, Savage VM, West GB (2004) Toward a metabolic theory of  
 721 ecology. *Ecology*, **85**, 1771-1789.
- 722 Bulleri F, Benedetti-Cecchi L, Acunto S, Cinelli F, Hawkins SJ (2002) The influence of canopy algae  
 723 on vertical patterns of distribution of low-shore assemblages on rocky coasts in the northwest  
 724 Mediterranean. *Journal of Experimental Marine Biology and Ecology*, **267**, 89-106.
- 725 Byrne M, Gonzalez-Bernat M, Doo S, Foo S, Soars N, Lamare M (2013) Effects of ocean warming  
 726 and acidification on embryos and non-calcifying larvae of the invasive sea star *Patiriella*  
 727 *regularis*. *Marine Ecology Progress Series*, **473**, 235-246.
- 728 Calosi P, Bilton DT, Spicer JI (2008) Thermal tolerance, acclimatory capacity and vulnerability to  
 729 global climate change. *Biology Letters*, **4**, 99-102.
- 730 Calosi P, Rastrick SP, Lombardi C *et al.* (2013) Adaptation and acclimatization to ocean acidification  
 731 in marine ectotherms: an in situ transplant experiment with polychaetes at a shallow CO<sub>2</sub> vent  
 732 system. *Philosophical Transactions of the Royal Society B: Biological Sciences*, **368**,  
 733 20120444.
- 734 Cheung WW, Lam VW, Pauly D (2008) Modelling present and climate-shifted distribution of marine  
 735 fishes and invertebrates. *Fisheries Centre Research Reports*, **1198-6727**, **16(3)**.
- 736 Cheung WWL, Dunne J, Sarmiento JL, Pauly D (2011) Integrating ecophysiology and plankton  
 737 dynamics into projected maximum fisheries catch potential under climate change in the  
 738 Northeast Atlantic. *ICES Journal of Marine Science*, **68**, 1008–1018.
- 739 Cheung WWL, Lam VWY, Sarmiento JL, Kearney K, Watson R, Pauly D (2009) Projecting global  
 740 marine biodiversity impacts under climate change scenarios. *Fish and Fisheries*, **10**, 235–251.
- 741 Close C, Cheung W, Hodgson S, Lam V, Watson R, Pauly D (2006) Distribution ranges of  
 742 commercial fishes and invertebrates. *Fishes in Databases and Ecosystems. Fisheries Centre*  
 743 *Research Reports*, **14 (4)**.
- 744 Cripps IL, Munday PL, McCormick MI (2011) Ocean acidification affects prey detection by a  
 745 predatory reef fish. *PLoS ONE*, **6**, e22736.
- 746 Crothers J (1985) Dog-whelks: an introduction to the biology of *Nucella lapillus* (L.). *Field Studies*, **6**,  
 747 291-360.
- 748 De La Haye KL, Spicer JI, Widdicombe S, Briffa M (2012) Reduced pH sea water disrupts chemo-  
 749 responsive behaviour in an intertidal crustacean. *Journal of Experimental Marine Biology and*  
 750 *Ecology*, **412**, 134-140.
- 751 Dixson DL, Munday PL, Jones GP (2010) Ocean acidification disrupts the innate ability of fish to  
 752 detect predator olfactory cues. *Ecology Letters*, **13**, 68-75.
- 753 Doney SC, Fabry VJ, Feely RA, Kleypas JA (2009) Ocean acidification: the other CO<sub>2</sub> problem.  
 754 *Annual Review of Marine Science*, **1**, 169-192.
- 755 Eliason EJ, Clark TD, Hague MJ *et al.* (2011) Differences in thermal tolerance among sockeye  
 756 salmon populations. *Science*, **332**, 109-112.
- 757 Feely RA, Sabine CL, Lee K, Berelson W, Kleypas J, Fabry VJ, Millero FJ (2004) Impact of  
 758 anthropogenic CO<sub>2</sub> on the CaCO<sub>3</sub> system in the oceans. *Science*, **305**, 362-366.

759 Fernandes JA, Cheung WW, Jennings S *et al.* (2013) Modelling the effects of climate change on the  
760 distribution and production of marine fishes: accounting for trophic interactions in a dynamic  
761 bioclimate envelope model. *Global Change Biology*, **19**, 2596–2607.

762 Findlay HS, Beesley A, Dashfield S, Mcneill CL, Nunes J, Queirós AM, Woodward EMS (2013)  
763 UKOA Benthic Consortium, PML intertidal mesocosm experimental environment dataset.  
764 (ed Laboratory PM), British Oceanographic Data Centre - Natural Environment Research  
765 Council, UK.

766 Findlay HS, Kendall MA, Spicer JI, Turley C, Widdicombe S (2008) Novel microcosm system for  
767 investigating the effects of elevated carbon dioxide and temperature on intertidal organisms.  
768 *Aquatic Biology*, **3**, 51-62.

769 Findlay HS, Kendall MA, Spicer JI, Widdicombe S (2010) Relative influences of ocean acidification  
770 and temperature on intertidal barnacle post-larvae at the northern edge of their geographic  
771 distribution. *Estuarine, Coastal and Shelf Science*, **86**, 675-682.

772 Findlay HS, Wood HL, Kendall MA, Spicer JI, Twitchett RJ, Widdicombe S (2011) Comparing the  
773 impact of high CO<sub>2</sub> on calcium carbonate structures in different marine organisms. *Marine  
774 Biology Research*, **7**, 565-575.

775 Form AU, Riebesell U (2012) Acclimation to ocean acidification during long-term CO<sub>2</sub> exposure in  
776 the cold-water coral *Lophelia pertusa*. *Global Change Biology*, **18**, 843-853.

777 Harley CD (2011) Climate change, keystone predation, and biodiversity loss. *Science*, **334**, 1124-  
778 1127.

779 Harvey BP, Gwynn-Jones D, Moore PJ (2013) Meta-analysis reveals complex marine biological  
780 responses to the interactive effects of ocean acidification and warming. *Ecology and  
781 Evolution*, **3**, 1016-1030.

782 Harvey HW (1955) *Chemistry and fertility of sea waters*, Cambridge; University Press.

783 Helmuth BS, Hofmann GE (2001) Microhabitats, thermal heterogeneity, and patterns of physiological  
784 stress in the rocky intertidal zone. *The Biological Bulletin*, **201**, 374-384.

785 Hughes RN, Elner R (1979) Tactics of a predator, *Carcinus maenas*, and morphological responses of  
786 the prey, *Nucella lapillus*. *The Journal of Animal Ecology*, 65-78.

787 Ipc (2007) *Climate Change 2007: The Physical Science Basis*. (eds Solomon S, Qin D, Manning M,  
788 Chen Z, Marquis M, Averyt KB, Tignor M, Miller HL), Cambridge, United Kingdom and  
789 New York, NY, USA.

790 Ipc (2013) *Climate Change 2013: The Physical Science Basis*. (eds Stocker TF, Qin D, Plattner G-  
791 K, Tignor M, Allen SK, Boschung J, Nauels A, Y. Xia, Bex V, Midgley PM), Cambridge,  
792 United Kingdom and New York, NY, USA, **in press**.

793 Jennings S, Mélin F, Blanchard JL, Forster RM, Dulvy NK, Wilson RW (2008) Global-scale  
794 predictions of community and ecosystem properties from simple ecological theory.  
795 *Proceedings of the Royal Society B: Biological Sciences*, **275**, 1375-1383.

796 Johannesen A, Dunn AM, Morrell LJ (2012) Olfactory cue use by three-spined sticklebacks foraging  
797 in turbid water: prey detection or prey location? *Animal Behaviour*, **84**, 151-158.

798 Jørgensen C, Peck MA, Antognarelli F *et al.* (2012) Conservation physiology of marine fishes:  
799 advancing the predictive capacity of models. *Biology Letters*, **8**, 900-903.

800 Kearney M, Porter W (2009) Mechanistic niche modelling: combining physiological and spatial data  
801 to predict species' ranges. *Ecology Letters*, **12**, 334-350.

802 Kroeker KJ, Kordas RL, Crim R *et al.* (2013) Impacts of ocean acidification on marine organisms:  
803 quantifying sensitivities and interaction with warming. *Global Change Biology*, **19**, 1884-  
804 1896.

805 Landes A, Zimmer M (2012) Acidification and warming affect both a calcifying predator and prey,  
806 but not their interaction. *Marine Ecology Progress Series*, **450**, 1-10.

807 Mac Nally R (2000) Regression and model-building in conservation biology, biogeography and  
808 ecology: the distinction between—and reconciliation of—‘predictive’ and ‘explanatory’ models.  
809 *Biodiversity & Conservation*, **9**, 655-671.

810 Manríquez PH, Jara ME, Mardones ML *et al.* (2013) Ocean Acidification Disrupts Prey Responses to  
811 Predator Cues but Not Net Prey Shell Growth in *Concholepas concholepas* (loco). *PLoS ONE*,  
812 **8**, e68643.

- 813 Mcdonald MR, McClintock JB, Amsler CD, Rittschof D, Angus RA, Orihuela B, Lutostanski K  
814 (2009) Effects of ocean acidification over the life history of the barnacle *Amphibalanus*  
815 *amphitrite*. *Mar Ecol Prog Ser*, **385**, 179-187.
- 816 Menge BA, Branch GM (2001) Rocky intertidal communities. In: *Marine community ecology*. (eds  
817 Bertness MD, Gaines SD, Hay ME) pp 221–252. Sunderland, Massachusetts, USA, Sinauer  
818 Associates.
- 819 Metcalfe J, Le Quesne W, Cheung W, Righton D (2012) Conservation physiology for applied  
820 management of marine fish: an overview with perspectives on the role and value of telemetry.  
821 *Philosophical Transactions of the Royal Society B: Biological Sciences*, **367**, 1746-1756.
- 822 Mieszowska N, Sugden H, Firth L, Hawkins SJ (*In press*) The role of sustained observations in  
823 tracking impacts of environmental change on marine biodiversity and ecosystems.  
824 *Philosophical Transactions of the Royal Society A*.
- 825 Norman-López A, Plagányi É, Skewes T, Poloczanska E, Dennis D, Gibbs M, Bayliss P (2013)  
826 Linking physiological, population and socio-economic assessments of climate-change impacts  
827 on fisheries. *Fisheries Research*, **148**, 18-26.
- 828 Parker LM, Ross PM, O'connor WA, Pörtner HO, Scanes E, Wright JM (2013) Predicting the  
829 response of molluscs to the impact of ocean acidification. *Biology*, **2**, 651-692.
- 830 Pörtner HO, Knust R (2007) Climate change affects marine fishes through the oxygen limitation of  
831 thermal tolerance. *Science*, **315**, 95-97.
- 832 Rastrick S, Whiteley N (2011) Congeneric amphipods show differing abilities to maintain metabolic  
833 rates with latitude. *Physiological and Biochemical Zoology*, **84**, 154-165.
- 834 Raymond CM, Bryan BA, Macdonald DH, Cast A, Strathearn S, Grandgirard A, Kalivas T (2009)  
835 Mapping community values for natural capital and ecosystem services. *Ecological*  
836 *Economics*, **68**, 1301-1315.
- 837 Reipschläger A, Nilsson GE, Pörtner H-O (1997) A role for adenosine in metabolic depression in the  
838 marine invertebrate *Sipunculus nudus*. *American journal of physiology-regulatory integrative*  
839 *and comparative physiology*, **272**, R350-R356.
- 840 Rodolfo-Metalpa R, Houlbrèque F, Tambutté É *et al.* (2011) Coral and mollusc resistance to ocean  
841 acidification adversely affected by warming. *Nature Climate Change*, **1**, 308-312.
- 842 Schaum CE, Batty R, Last KS (2013) Smelling Danger—Alarm Cue Responses in the Polychaete  
843 *Nereis* (*Hediste*) *diversicolor* (Müller, 1776) to Potential Fish Predation. *PLoS ONE*, **8**,  
844 e77431.
- 845 Seed R (1996) Patterns of biodiversity in the macro-invertebrate fauna associated with mussel patches  
846 on rocky shores. *Journal of the Marine Biological Association of the United Kingdom*, **76**,  
847 203-210.
- 848 Selin N (2010) Peculiarities of the habitat of *Nucella freycineti* (Mollusca: Gastropoda) at  
849 volcanogenic vent sites. *Russian Journal of Marine Biology*, **36**, 26-33.
- 850 Shutler J, Smyth T, Saux-Picart S *et al.* (2011) Evaluating the ability of a hydrodynamic ecosystem  
851 model to capture inter-and intra-annual spatial characteristics of chlorophyll-*a* in the  
852 north east Atlantic. *Journal of Marine Systems*, **88**, 169-182.
- 853 Thomsen J, Casties I, Pansch C, Körtzinger A, Melzner F (2013) Food availability outweighs ocean  
854 acidification effects in juvenile *Mytilus edulis*: laboratory and field experiments. *Global*  
855 *Change Biology*, **19**, 1017-1027.
- 856 Trussell GC, Ewanchuk PJ, Bertness MD (2003) Trait-mediated effects in rocky intertidal food  
857 chains: predator risk cues alter prey feeding rates. *Ecology*, **84**, 629-640.
- 858 Vadas RS, Burrows M, Hughes R (1994) Foraging strategies of dogwhelks, *Nucella lapillus* (L.):  
859 interacting effects of age, diet and chemical cues to the threat of predation. *Oecologia*, **100**,  
860 439-450.
- 861 Watson S-A, Lefevre S, McCormick MI, Domenici P, Nilsson GE, Munday PL (2014) Marine mollusc  
862 predator-escape behaviour altered by near-future carbon dioxide levels. *Proceedings of the*  
863 *Royal Society B: Biological Sciences*, **281**, 20132377.
- 864 Wernberg T, Smale DA, Thomsen MS (2012) A decade of climate change experiments on marine  
865 organisms: procedures, patterns and problems. *Global Change Biology*, **18**, 1491-1498.

866 Yool A, Popova EE, Coward AC, Bernie D, Anderson TR (2013) Climate change and ocean  
867 acidification impacts on lower trophic levels and the export of organic carbon to the deep  
868 ocean. *Biogeosciences Discussions*, **10**, 3455-3522.

869

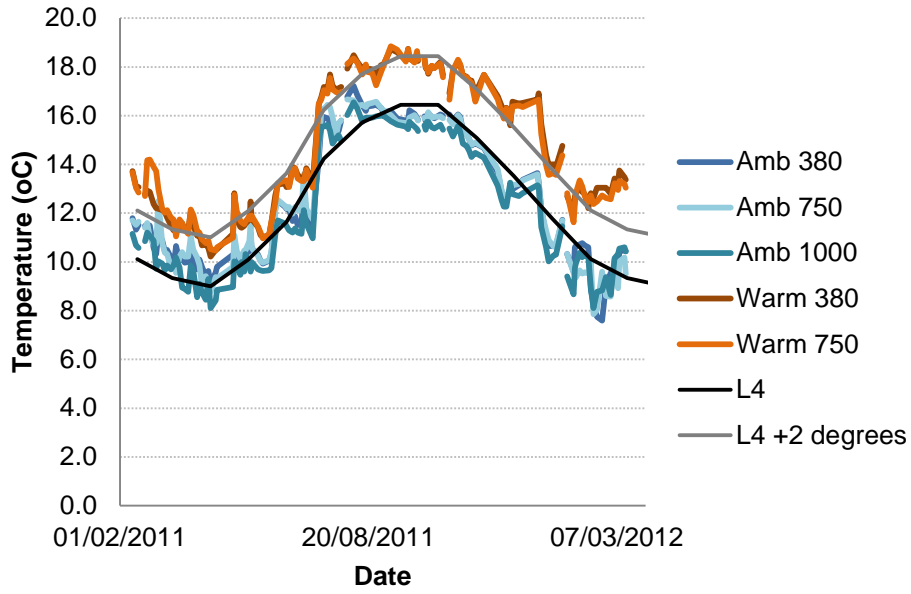
870

871 **Supporting Information**

872 **Table SI:** Carbonate chemistry parameters (mean  $\pm$  standard deviation) measured during the mesocosm experiments, averaged across replicate  
 873 tanks.  $A_T$ : total alkalinity; pH: total hydrogen ion concentration; Temp: temperature; Sal: salinity; DIC: total dissolved inorganic carbon;  $pCO_2$ :  
 874 the partial pressure of  $CO_2$  in seawater;  $\Omega_{Calc}$ : the saturation state of seawater for calcite;  $\Omega_{Arag}$ : the saturation state of seawater for aragonite;  
 875  $HCO_3^-$ : the bicarbonate ion concentration;  $CO_3^{2-}$ : the carbonate ion concentration.

nominal treatment	$A_T$ ( $\mu\text{mol kg}^{-1}$ )	pH	Temp ( $^{\circ}\text{C}$ )	Sal (psu)	DIC ( $\mu\text{mol.kg}^{-1}$ )	$pCO_2$ ( $\mu\text{atm}$ )	$\Omega_{Calc}$	$\Omega_{Arag}$	$HCO_3^-$ ( $\mu\text{mol.kg}^{-1}$ )	$CO_3^{2-}$ ( $\mu\text{mol.kg}^{-1}$ )
<b>380 Ambient</b>	2205.75 $\pm$ 83.69	8.03 $\pm$ 0.08	11.78 $\pm$ 2.01	34.82 $\pm$ 0.32	2064.42 $\pm$ 70.45	540.64 $\pm$ 121.15	2.57 $\pm$ 0.52	1.64 $\pm$ 0.33	1934.08 $\pm$ 66.61	107.88 $\pm$ 21.81
<b>750 Ambient</b>	2166.35 $\pm$ 82.61	7.93 $\pm$ 0.09	11.62 $\pm$ 2.29	34.80 $\pm$ 0.28	2064.45 $\pm$ 83.06	689.44 $\pm$ 158.88	2.03 $\pm$ 0.37	1.30 $\pm$ 0.24	1950.59 $\pm$ 82.30	85.25 $\pm$ 15.59
<b>1000 Ambient</b>	2306.77 $\pm$ 9.52	7.79 $\pm$ 0.08	11.48 $\pm$ 2.26	34.88 $\pm$ 0.30	2247.13 $\pm$ 85.38	1020.19 $\pm$ 196.43	1.62 $\pm$ 0.27	1.03 $\pm$ 0.17	2136.45 $\pm$ 83.45	68.03 $\pm$ 11.23
<b>380 Warm</b>	2252.24 $\pm$ 111.75	8.00 $\pm$ 0.09	13.98 $\pm$ 2.31	35.00 $\pm$ 0.25	2109.48 $\pm$ 133.69	611.64 $\pm$ 165.74	2.63 $\pm$ 0.43	1.70 $\pm$ 0.28	1975.26 $\pm$ 139.58	110.44 $\pm$ 18.09
<b>750 Warm</b>	2228.72 $\pm$ 114.03	7.90 $\pm$ 0.10	13.95 $\pm$ 2.27	35.05 $\pm$ 0.24	2124.05 $\pm$ 130.11	791.48 $\pm$ 232.61	2.12 $\pm$ 0.42	1.36 $\pm$ 0.27	2004.29 $\pm$ 131.76	89.11 $\pm$ 17.69

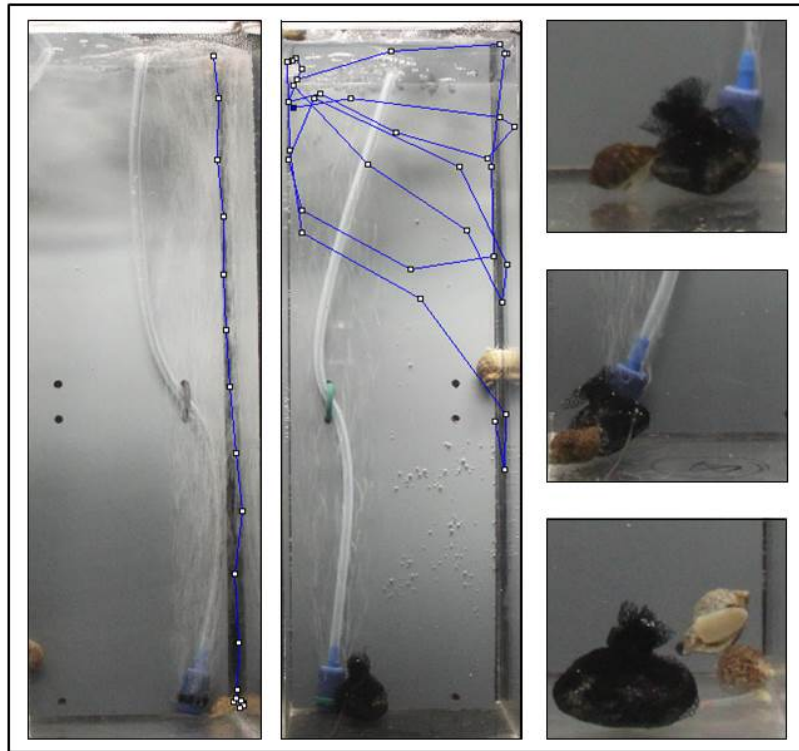
876



877

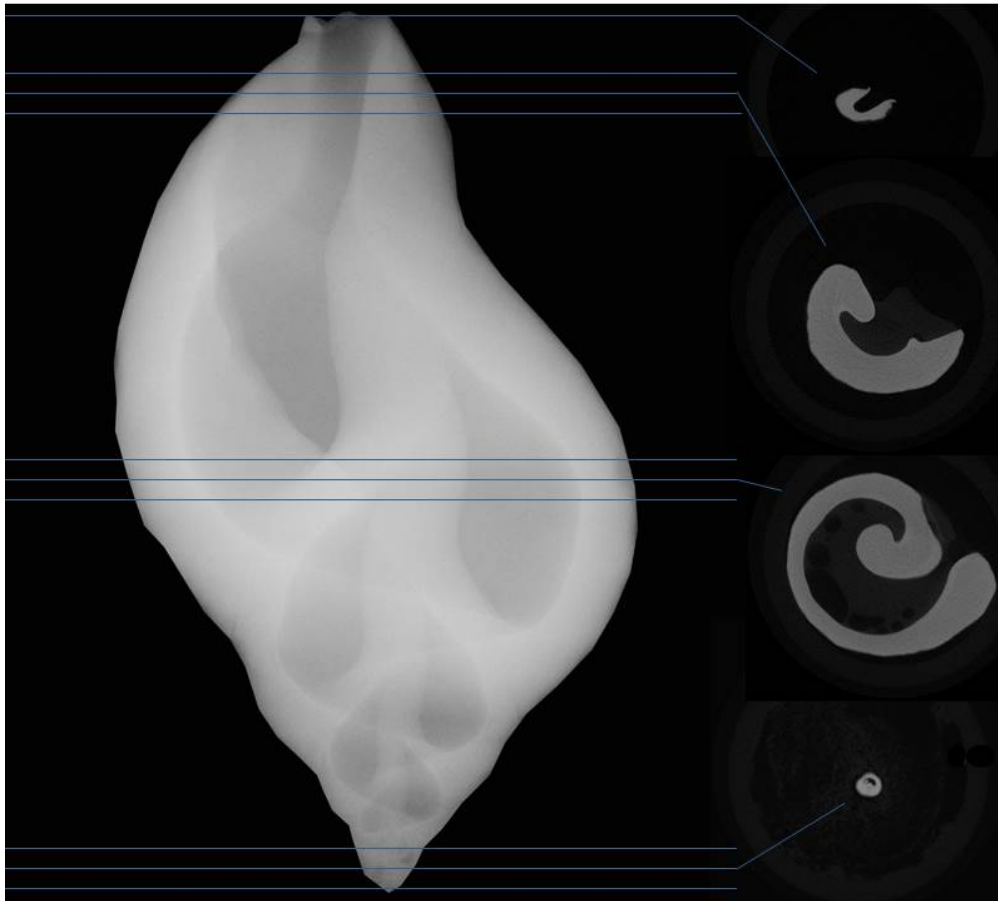
878 **Figure S1:** Temperature variation at the L4 station in the Plymouth Sound, and in our  
 879 experimental treatments, over the duration of the mesocosm exposures.

880



881  
 882 **Figure S2:** Activity and predatory behaviour assessments. Left panel showing the trajectory  
 883 of an individual (dotted line) from the bottom of the tank to the water line, during an activity  
 884 assessment at ambient temperature and high CO<sub>2</sub> (1000 ppm). The speed of the first  
 885 individual to reach the waterline in each assessment was taken as a proxy for basal activity.  
 886 Centre panel shows the trajectory of an individual in an ambient temperature and medium  
 887 CO<sub>2</sub> treatment (dotted line) after the addition of a prey mimic to the tank (black, bottom left).  
 888 This individual has failed to find the prey mimic. Right panel shows individuals handling the  
 889 prey mimic during predatory behaviour assessments at ambient temperature and (top to  
 890 bottom) 380, 750 and 1000 ppm of CO<sub>2</sub>.

891

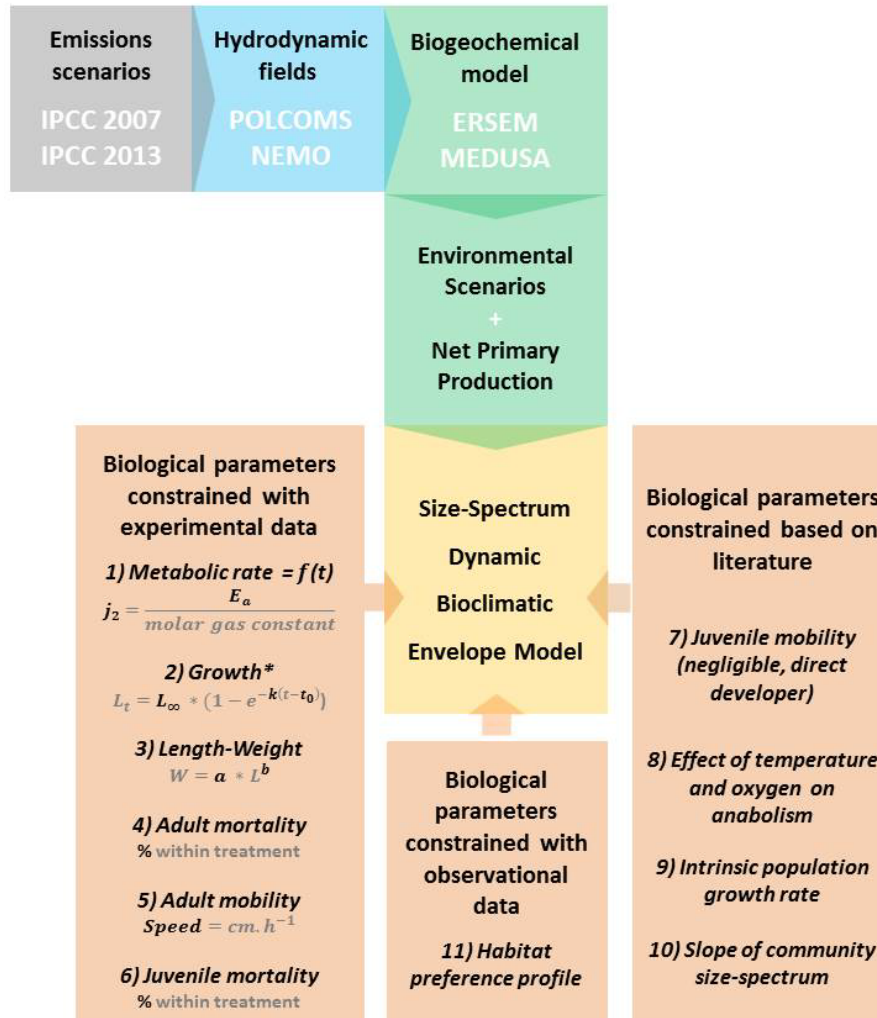


892

893 **Figure S3:** Micro-CT data extraction. Position (left, lines) of the ten shell slices (right, raw  
894 data) acquired with microCT and analysed in the estimation of shell surface density. Top line  
895 indicates the position of the slice (top right) used for the calculation of shell lip density.

896





898

899 **Figure S4:** Schematic diagram of the SS-DBEM structure, indicating which parameters were  
 900 estimated based on experimental and observational data, in the present study. Based on  
 901 Fernandes et al. (2013) and Cheung et al.(2011) . \* Please refer to text for detail about growth  
 902 calculations.

903

904

905

906 **Tables**

907

908 **Table I:** Regression models for responses of activity and predatory behaviour to experimental  
 909 treatments, after fourteen month long mesocosm exposures to ocean acidification and  
 910 warming (S.I. 2). Model selection was carried out using a log-likelihood based stepwise  
 911 procedure. “NA” model structure indicates response variables for which none of the  
 912 experimental factors and covariate considered provided a better fit than the null model. “df”:  
 913 degrees of freedom.

	Variable	Model structure	df	F	p	R <sup>2</sup> (%)
Basal activity	speed	CO <sub>2</sub> concentration	2, 22	5.21	< 0.05	32.15
	response time	NA	24	0.00	> 0.05	NA
Predatory behaviour	foraging distance	CO <sub>2</sub> concentration x tide	3,23	4.99	<0.01	39.41
	foraging cost	~ CO <sub>2</sub> concentration	2,9	4.93	<0.05	52.30

914 \* Animals only actively sought food at high tide.

915

916 **Figure Legends**

917 **Figure 1:** Effects of ocean acidification and warming on individual level responses (a and b)  
918 and predatory behaviour (c-f) after fourteen month long experimental exposures.

919 **Figure 2:** Micro-CT reconstructions of *Nucella lapillus* shells. Top panel: 3D reconstructions  
920 of individuals from control treatments (top row), exhibiting normal, reticulated shell  
921 ornamentation. Bottom row shows individuals from the most extreme acidification treatments  
922 exhibiting loss of natural ornamentation pattern, worn apex and shallow whorl definition  
923 (arrows). Bottom panel: 2D detail of inter-calibrated cross-sections of the lip of the shell of  
924 control individuals (top row) and from ambient 1000 ppm CO<sub>2</sub> treatment (bottom), using a 16  
925 colour mask to enhance differences in shell density. Warm colours indicate high density  
926 materials (yellow) and cold colours (blue) indicate low density.

927 **Figure 3:** SS-DBEM biogeographical projections for *Nucella lapillus* abundance in the  
928 present (1986-2000, left, a, e, and i); and future (2086-2100, all other columns), when model  
929 parameters are adjusted to respond to changes in temperature (second from left, b, f and j),  
930 ocean acidification (third from left, c, g and k) and both (right, d, h and l). The colouring of  
931 the plots is the fifteen year average within each cell, indicating abundance standardized  
932 relative to the present in scenario A1B (a), varying from 0 (white) to 1 (sky blue). The  
933 numbers plotted in red are the % change in *Nucella lapillus* abundance in the future scenarios  
934 in relation to the present distribution in each region (red lines), when model parameters  
935 respond to acidification and warming simultaneously. Rows correspond to model runs using:  
936 POLCOMS-ERSEM 4th IPCC special report emissions scenario A1B “business-as-usual”  
937 (top row, a-d); and NEMO-MEDUSA 2.0 using the 5<sup>th</sup> IPCC special report emissions  
938 scenarios AR5 RCP2.6 “lower emissions” (second row, e-h) and AR5 RCP8.5 “higher  
939 emissions” (bottom row, i-l).